Stability of Alfven modes and thermal plasma: the gyro-fluid code FAR3d

author:

Jacobo Varela Rodriguez

Co -author:

IFS: F. L. Waelbroeck, B. Breizman, D. Hatch, S. M. Mahajan, R. Fitzpatrick

ORNL: D. Spong, Y. Ghai, D. Del Castillo

UC3M: L. Garcia, J. Ortiz, J.M. Reynolds, R. Sanchez, V. Tribaldos and J. Solis

TJ-II: C. Hidalgo, A. Cappa, S. Melnikov, E. Ascacibar

DIII-D: M. Van Zeeland, A. M. Garofalo, D. Pace, W. W. Heidbrink, X. Du, Deyong

KSTAR: J. Kim and J. Kang

NIFS & CFQS: K.Y. Watanabe, K. Nagaoka, Y. Takemura, Y. Todo, T. Tokuzawa, K. Ida, A. Shimizu, R. Seki, Y. Suzuki, K. Tanaka

IPP: F. Jenko, A. Di Sienna and A. Knieps

Heliotron J: K. Nagasaki, S. Kobayashi

JT60SA: J. Garcia, K. Shinohara, J. Shiraishi, S. Yamamoto, M. Honda, A. Bierwage

EAST & CFEDR: J. Huang, V. Chan, X. Wang, Zhiyong Qiu

JET: S. Sharapov and M. Fitzgerald

Laboratoire M2P2 CNRS and CEA: D. Zarzoso and S. Mazzi

Universidad de Sevilla: M. Garcia-Munoz, J. Rueda.

INDEX

Motivation: EP destabilize the plasma

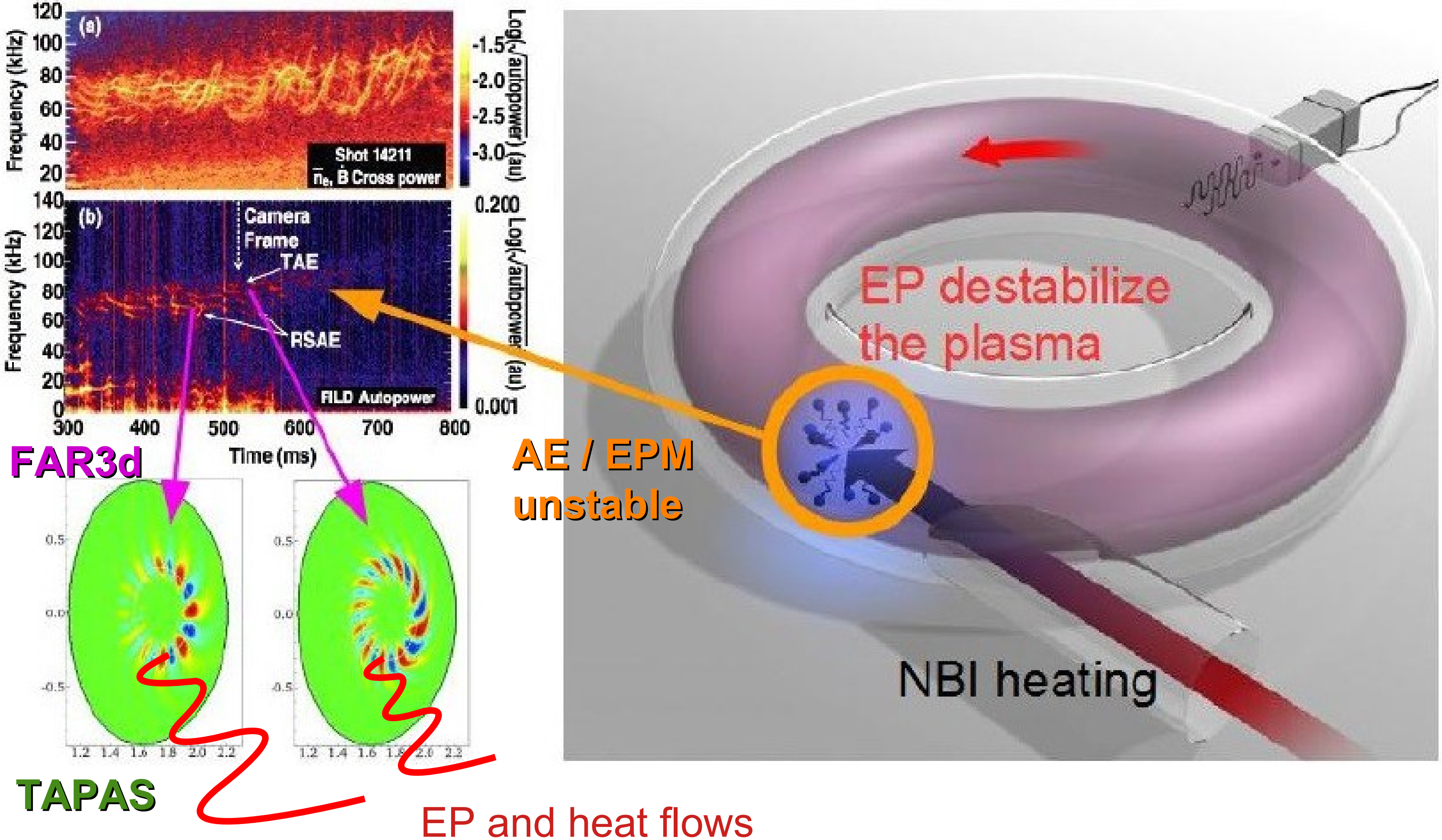

Motivation: How EP and AEs interact?

- AEs can be triggered if the EP velocity is similar to the MHD wave group velocity, that is to say, **a resonance takes place !!**

- Energetic particle (EP) driven instabilities can **enhance** the **transport** of fusion produced **alpha particles**, energetic neutral beam particles (**NBI driven EP**) and particles heated using ion cyclotron resonance heating (**ICRF driven EP**).

- **This is bad ? YES**

EP/alphas are lost before thermalization.

- **Consequences ?**

→ **Damage** of plasma-facing components.

→ **Inefficient** plasma heating.

→ **Increase** of the operation scenario **requirements**.

→ **Reduce or hamper** the **economic viability** of future **reactors**.

- **Something is missing in present day experiments ? YES**

Multiple EP populations will co-exist in reactor plasma leading to a **strong nonlinear coupling between EP species: AE stability is affected !!**

The gyro-fluid FAR3d code

Project overview: initial value FAR3d code

- Gyro fluid FAR3d code: fluid thermal plasma + EP perturbation

  - Reduced MHD + Moments of the gyro-kinetic equation (Landau closure -> gyro-kinetic eq. truncation).

  - Pressure/current gradient driven modes (including resistive MHD modes) + wave-particle resonance reproducing the Landau damping\growth.

- FAR3d code main features (linear and non linear):
  - 3d system (VMEC equilibria).
  - Toroidal and helical couplings.
  - Experimental profiles as input.
  - Multiple EP species.
  - Finite Larmor Radius (thermal + EP) and e-i Landau damping effects.
  - Eigensolver: sub-dominant modes.
  - Passing (tangential NBI) and trapped (perpendicular NBI) EPs.

Project overview: why a gyro-fluid code?

- Short simulation time (seconds for linear simulations):

  - Quick parametric studies.

  - Fast experimental data interpretation.

- Optimization:
  - NBI operational regime (EP β, energy and deposition region).
  - Magnetic field topology (NBI current drive and ECCD from VMEC).
  - Multiple EP population: **Multiple EP damping / drive effects.**
  - Thermal plasma density / temperature.

- Experiment interpretation:
  - AE characterization: AE family, dominant modes, eigenfunction, ...
  - MHD stability trends.
  - Dominant (highest growth rate) and sub-dominant modes.
  - Nonlinear MHD and wave-particle saturation phases: bursting, chirping, zonal flow, zonal currents, ...

Project overview: research strategy and geography

- Close collaboration with experimental research groups: theory and experiments must be directly connected !!
  - Reproduce the AE activity and identification of optimization trends.
  - Experiment proposals: DIII-D, LHD, EAST, TJ-II.
- Strong international collaborations:

- Open source code:
  - FAR3d distribution (linear version) available

Project overview: gyro-fluid vs gyro-kinetic

- Gyro-fluid and gyro-kinetic / hybrid approaches are complementary !!

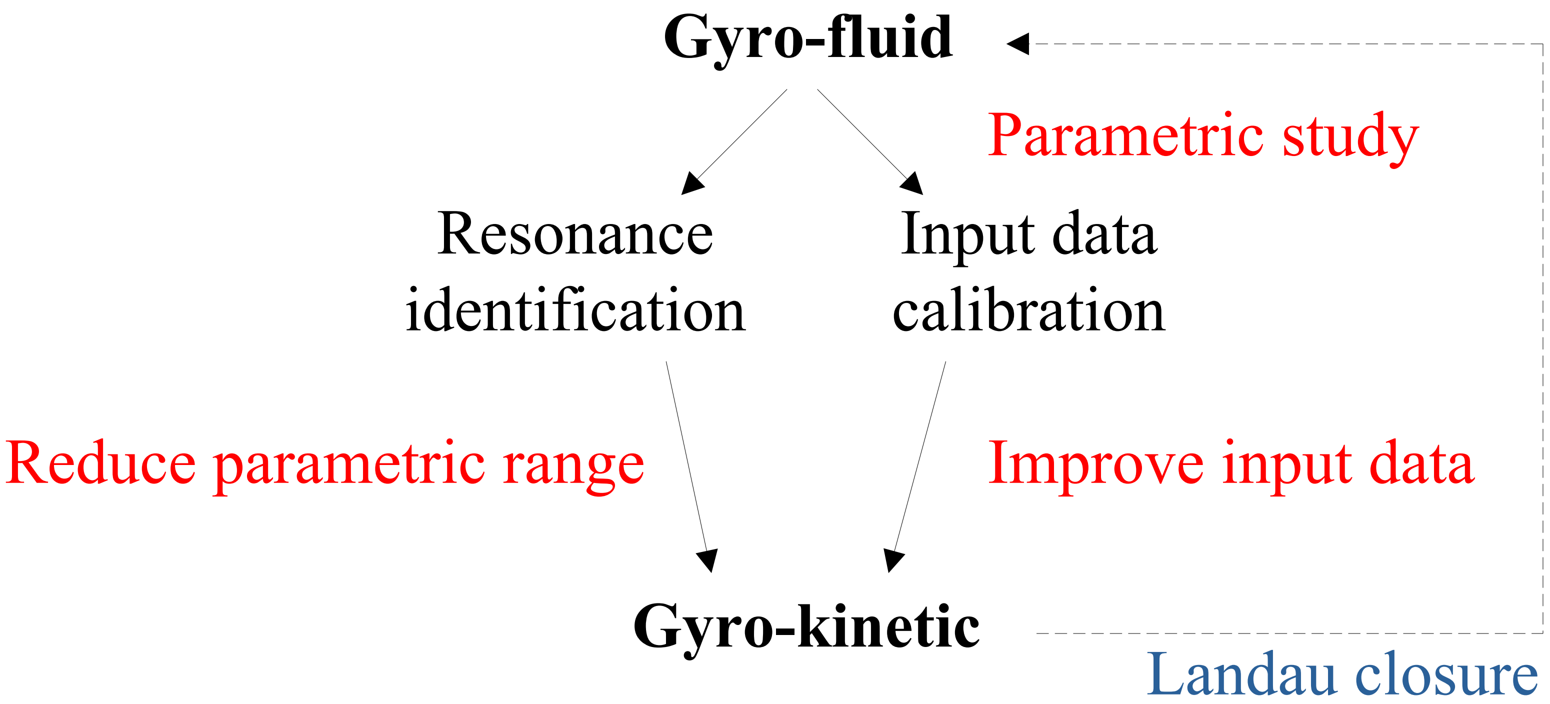

AE activity characterization

AE activity in DIII-D reverse shear discharges

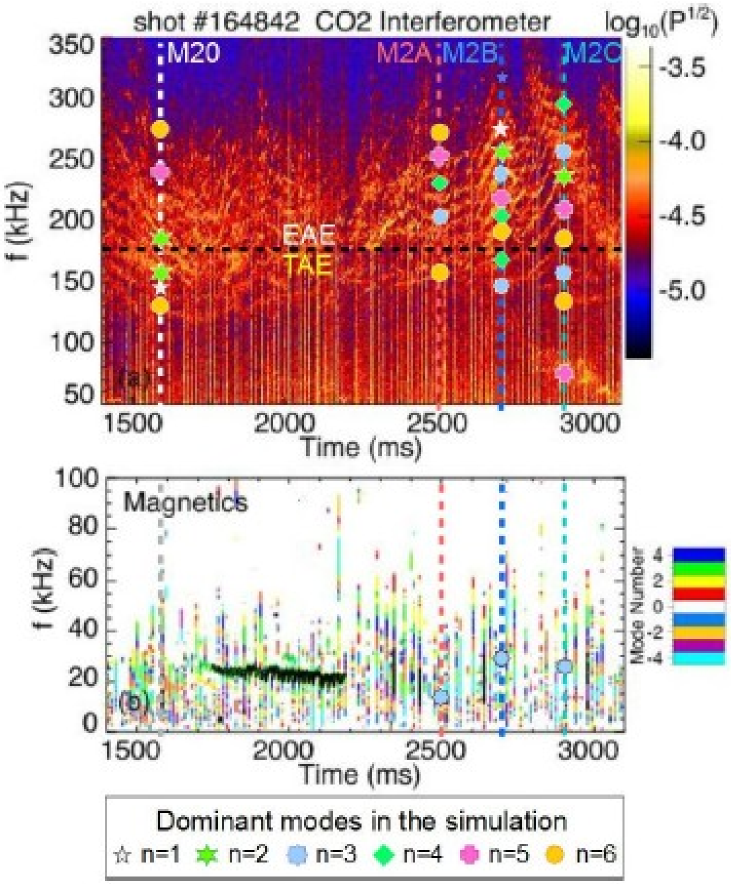

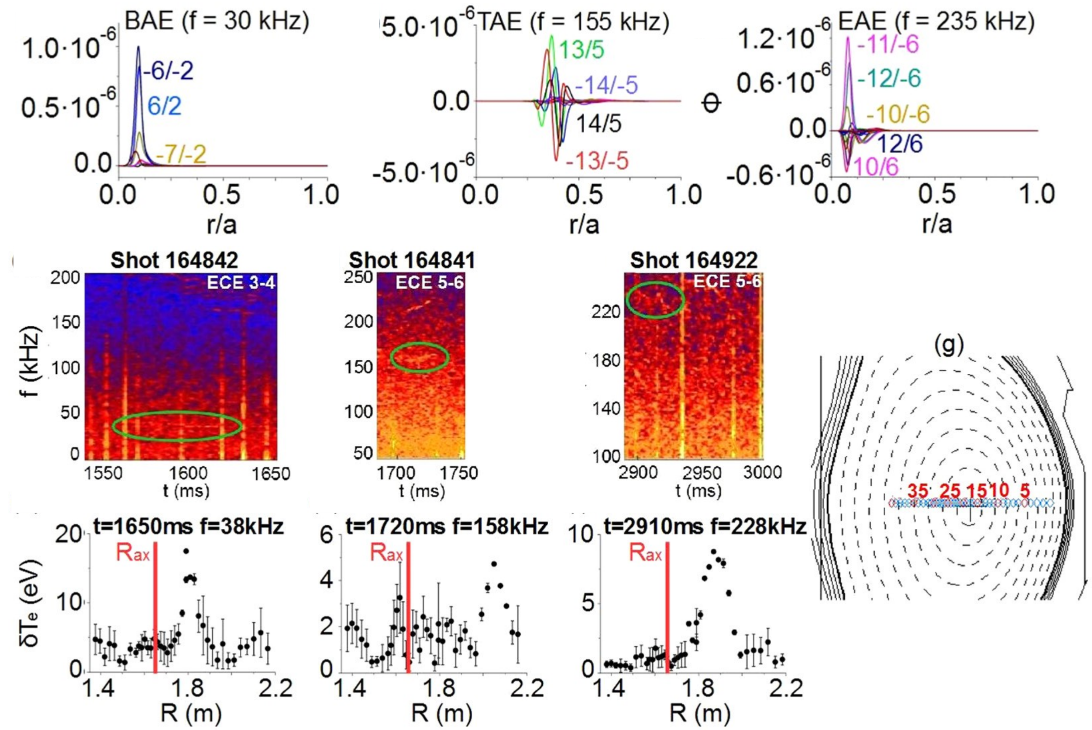

J. Varela et al, Nucl. Fusion 59 046017 (2019)

- Analysis of the AE activity along the discharge.
- Simulation AE frequency range, radial location, eigenfunction structure and dominant modes must be consistent with the observations.

AE activity in EAST after Tungsten contamination

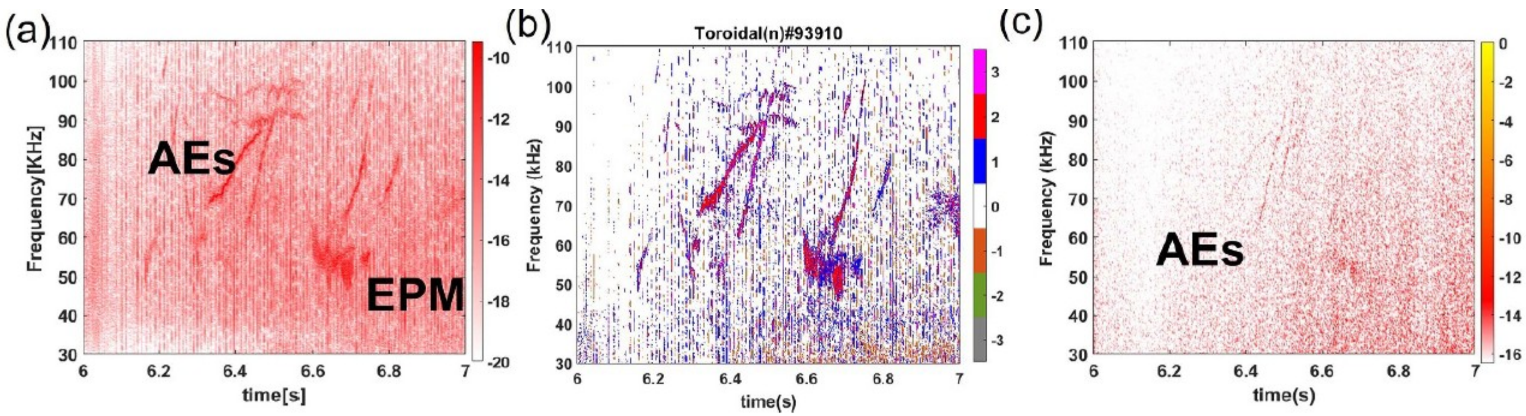

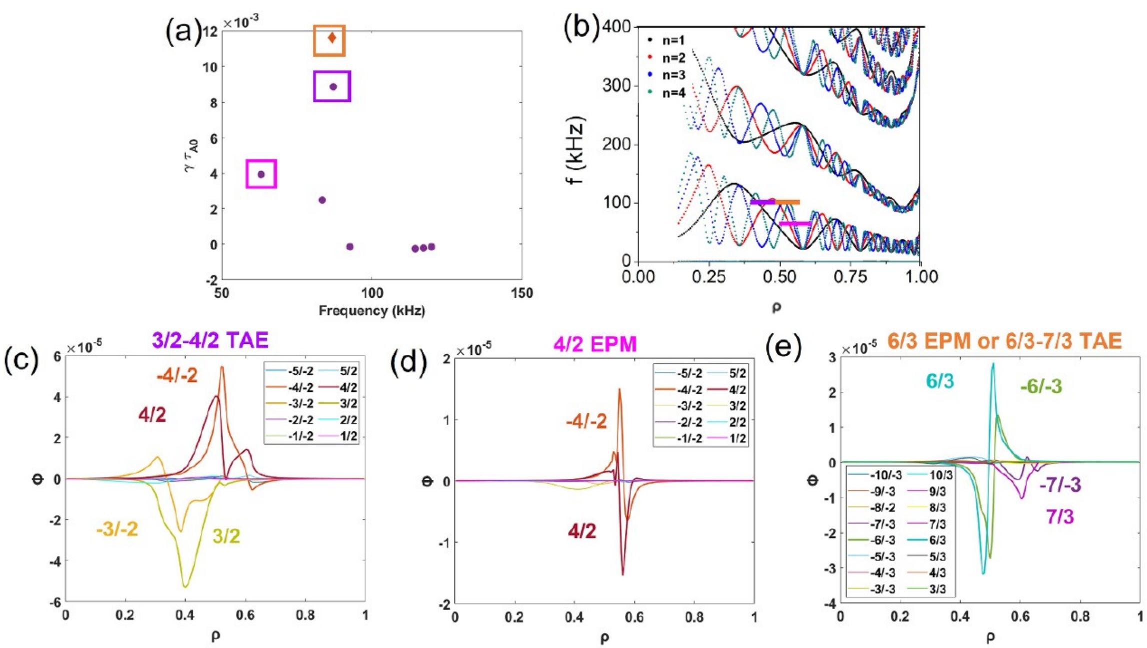

- AE / EPM activity observed in EAST is reproduced.

- AE / EPM destabilization explained:

=> Thermal ion density ↑.

=> Lower Alfven velocity.

=> EP resonance stronger.

X.H. Wang et al Nucl. Fusion 64 016028 (2024)

HAE and interchange mode stability in TJ-II

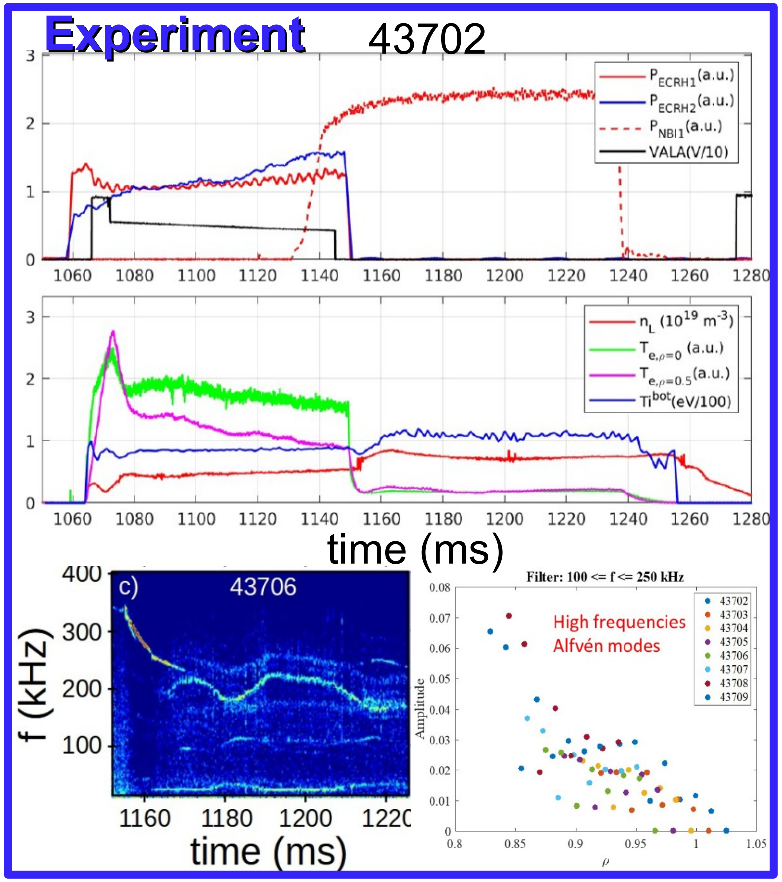

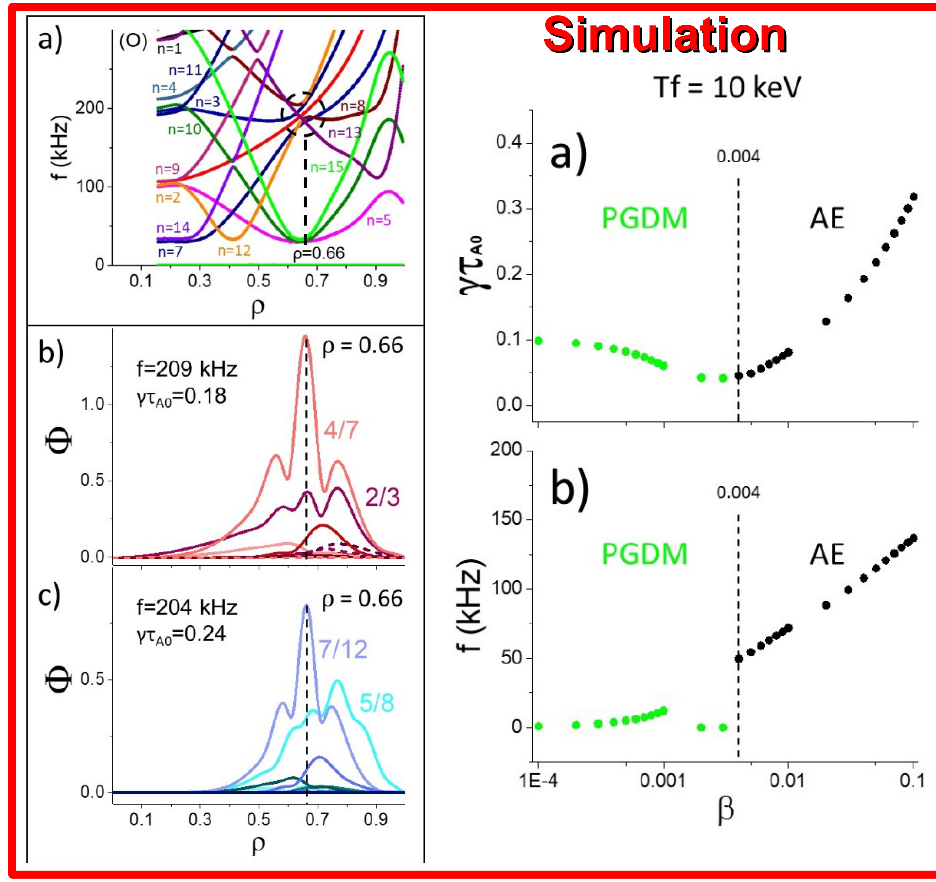

- AEs unstable in TJ-II periphery.

- HAEs identified in the plasma periphery. Analysis of stability trends for optimized NBI operational regime.

- Cross-stability effects AE and PGDM: EOs stabilizing effect on PGDM !!

J. Ortiz et al, poster, EPS 2023

AE activity in Heliotron J

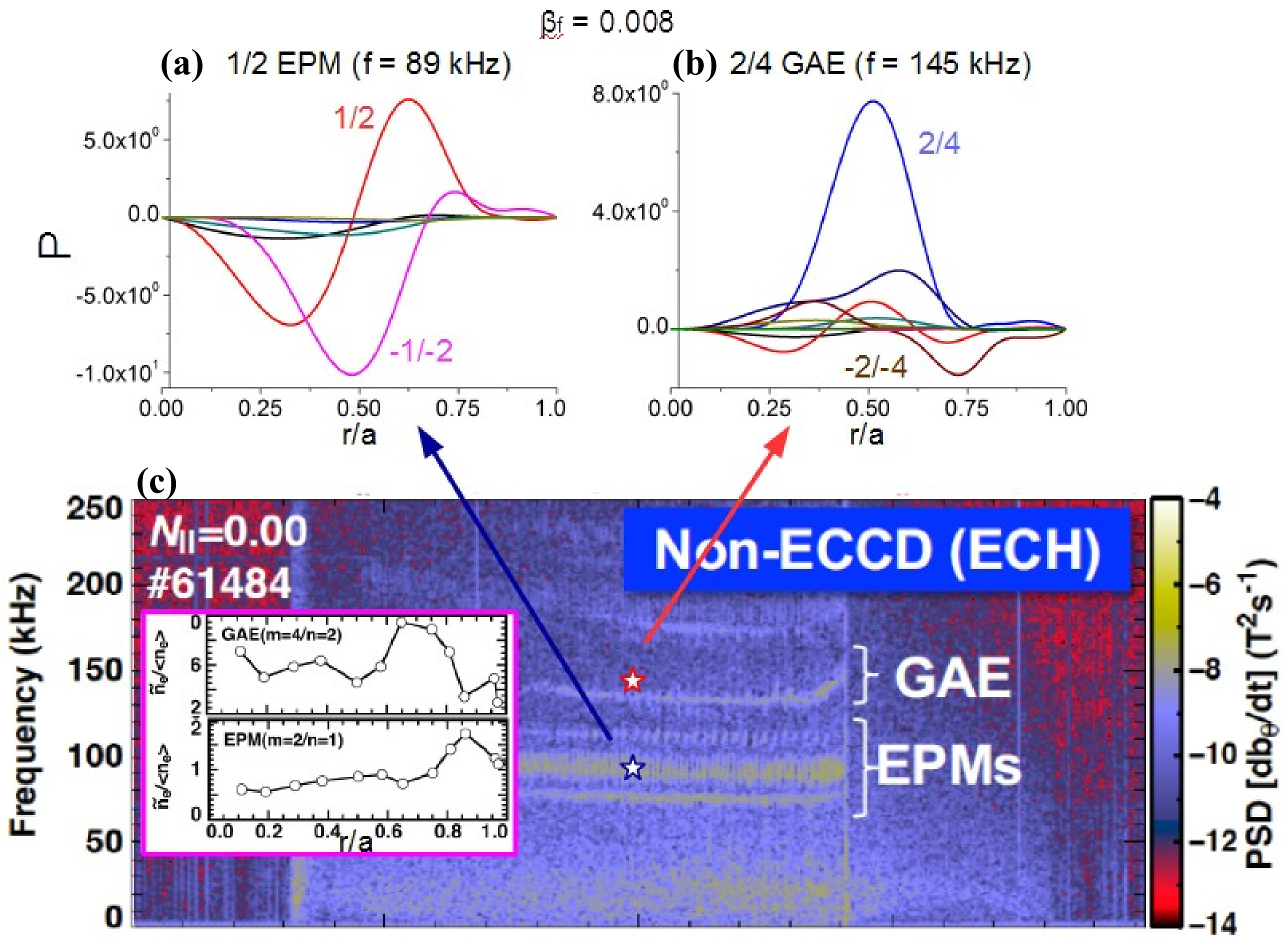

- The simulations identify the GAE and EPM observed in the experiment
- Correct radial location, frequency range and dominant modes.

S. Yamamoto et al, Nucl. Fusion 60 066018 (2020)

Plasma heating optimization

AE stabilization in LHD by the NBCD

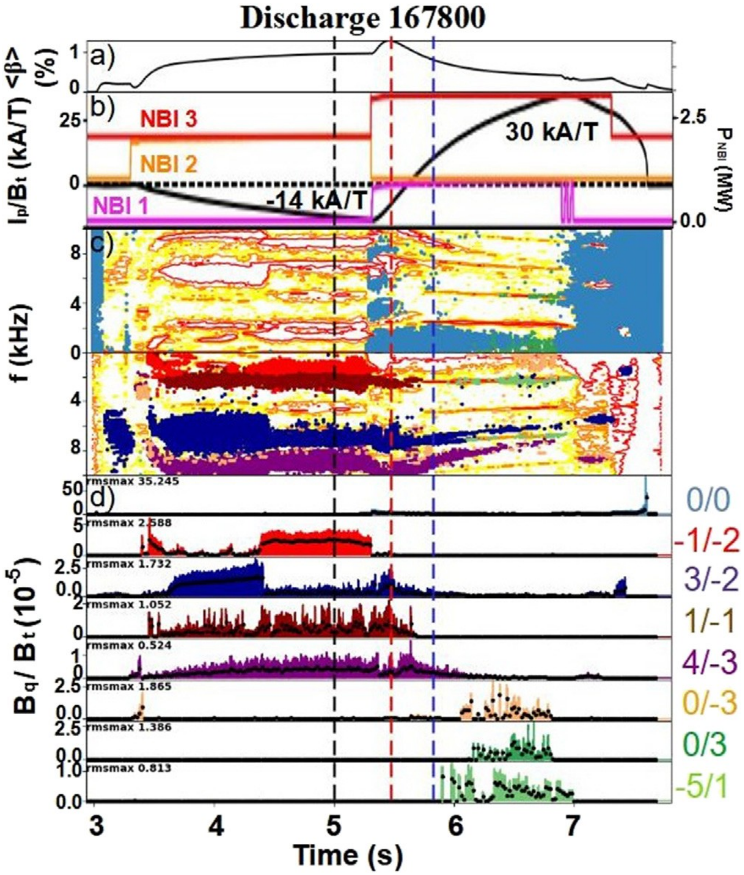

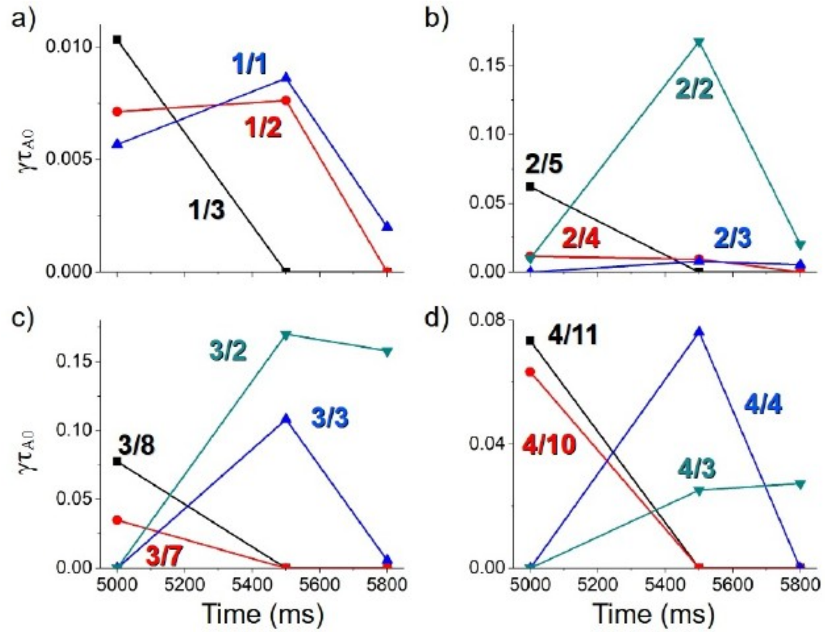

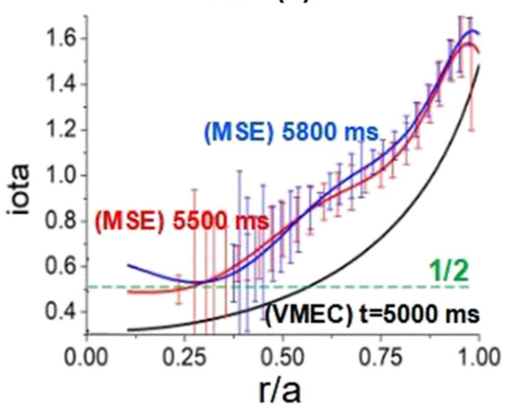

- Interchange mode 1/2 stabilized above a NBCD intensity thresholds

- Nonresonant transition 1/2 rational surface.

- MHD stability trends with respect to the NBCD iota variation reproduced numerically.

J. Varela et al, Phys. Plasmas 31, 082504 (2024)

AE stabilization in LHD by the NBCD

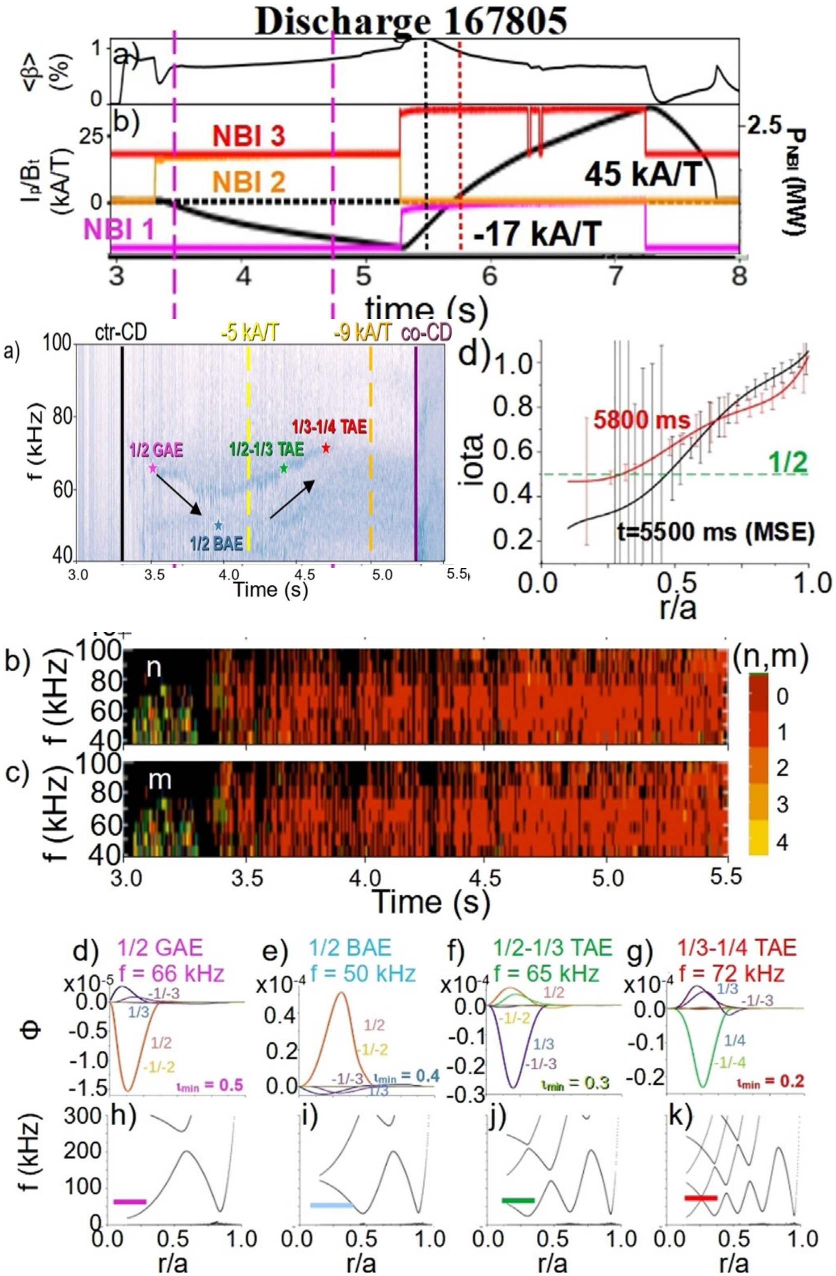

- Low density discharge: stable interchange modes (low thermal plasma β) but AEs unstable (strong EP resonance).

- AEs triggered during ctr-NBCD phase if NBCD intensity above 21 kA.

- MSE data: iota profile down-shift during ctr-NBI leads to a iota profile below 0.3.

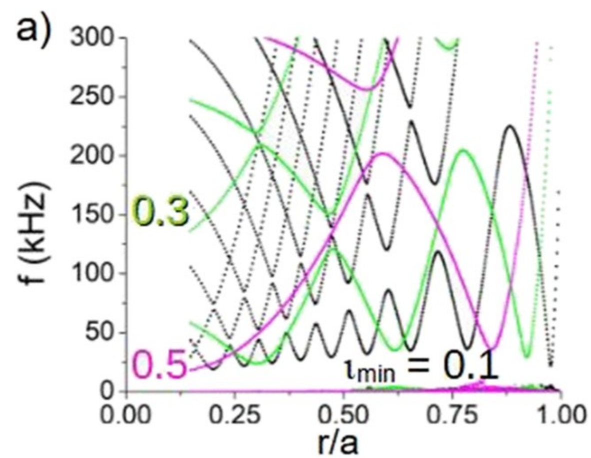

- Strong iota profile down-shift causes slender gaps: enhanced continuum damping.

J. Varela et al, Phys. Plasmas 31, 082504 (2024)

AE stabilization in LHD by the NBCD

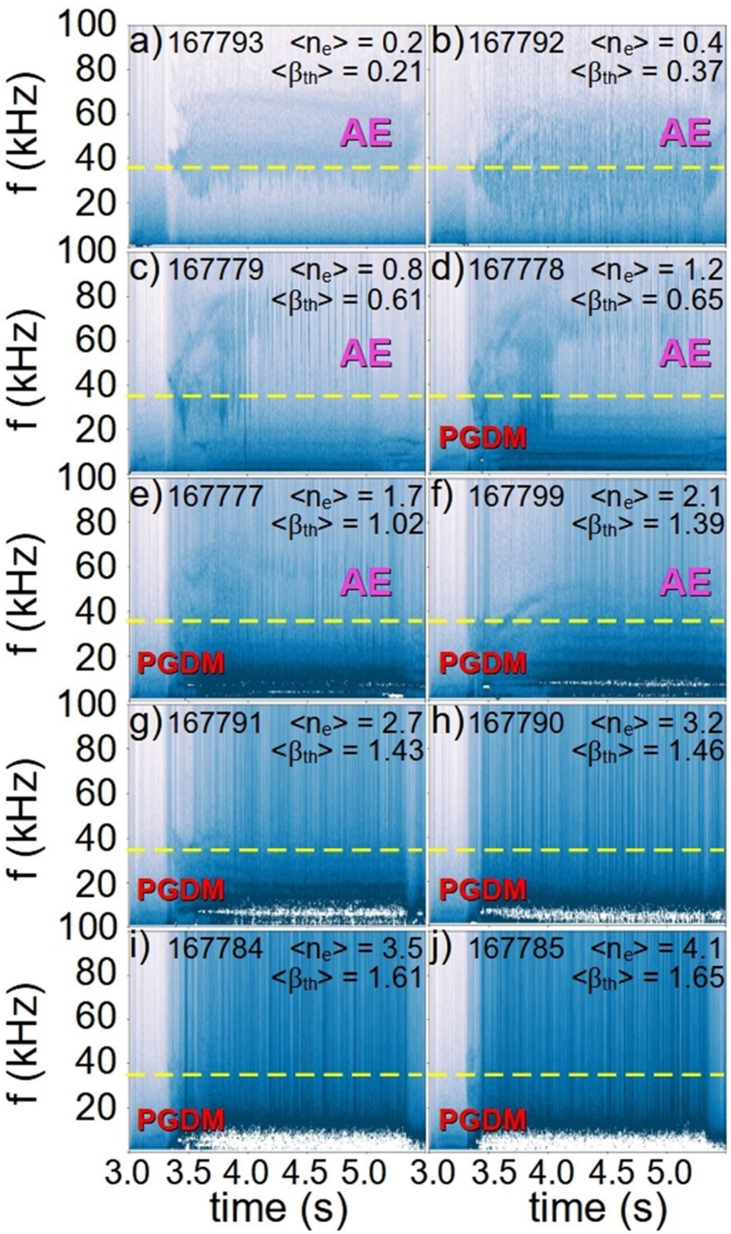

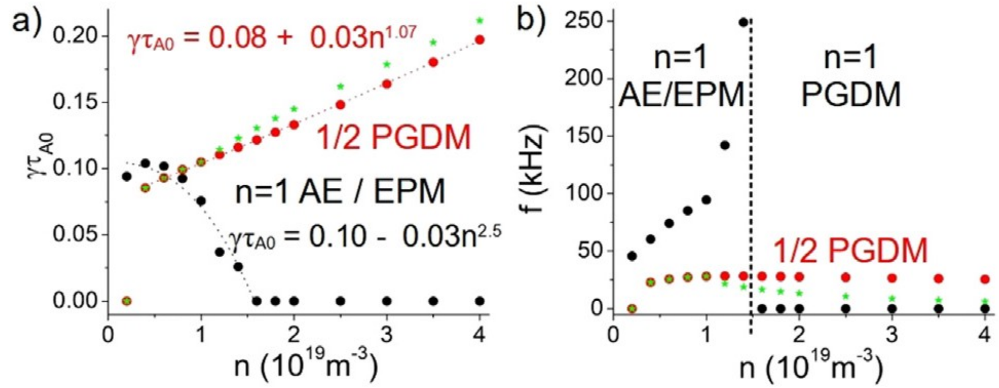

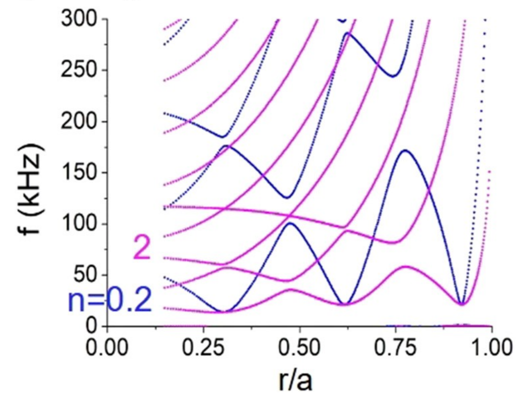

- Large thermal ion density discharges show lower AE activity: lower EP β (faster slowing down time), weaker resonance (lower Alfven velocity) and stronger continuum damping (slender gaps).

J. Varela et al, Phys. Plasmas 31, 082504 (2024)

Effect of the ECCD in the AE stability in LHD plasma

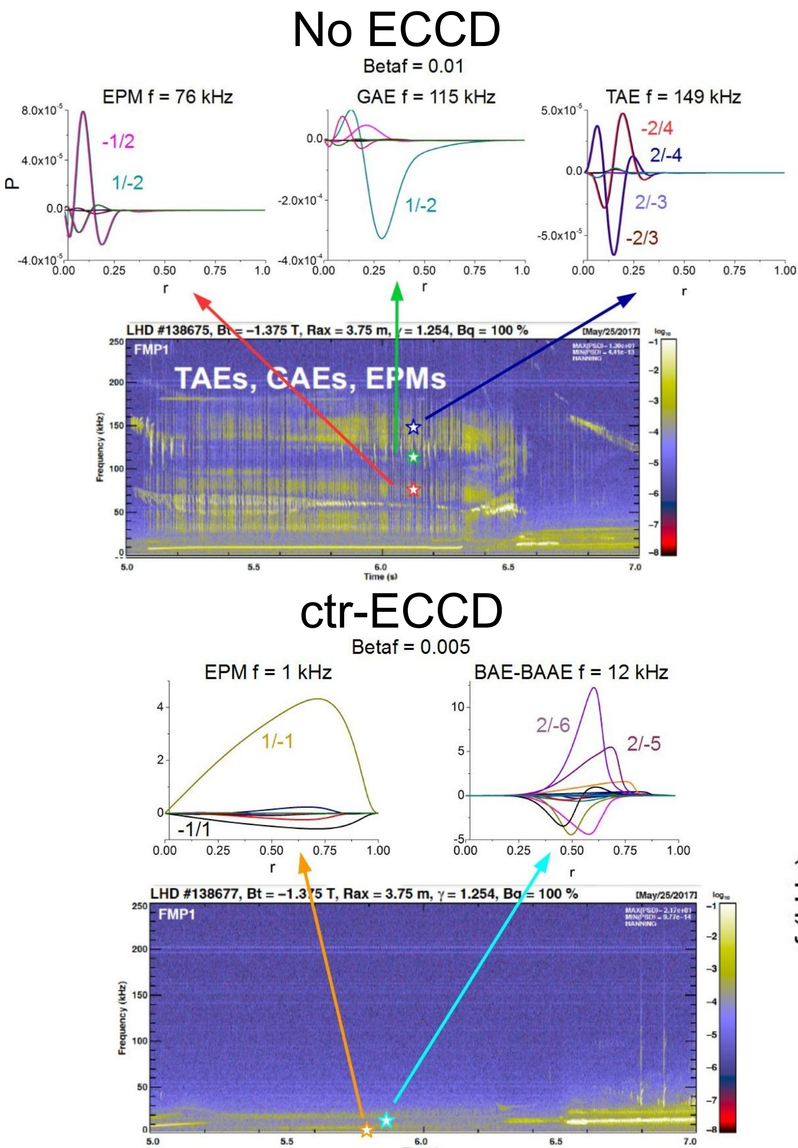

- Simulations reproduce the experiment observations: AEs stable if ctr-ECCD is injected in the plasma (fig 1 and 2).

- Ctr-ECCD: slender continuum gaps + stronger continuum damping (fig 3): AE stability improved.

J. Varela et al Nucl. Fusion, 60, 112015 (2020)

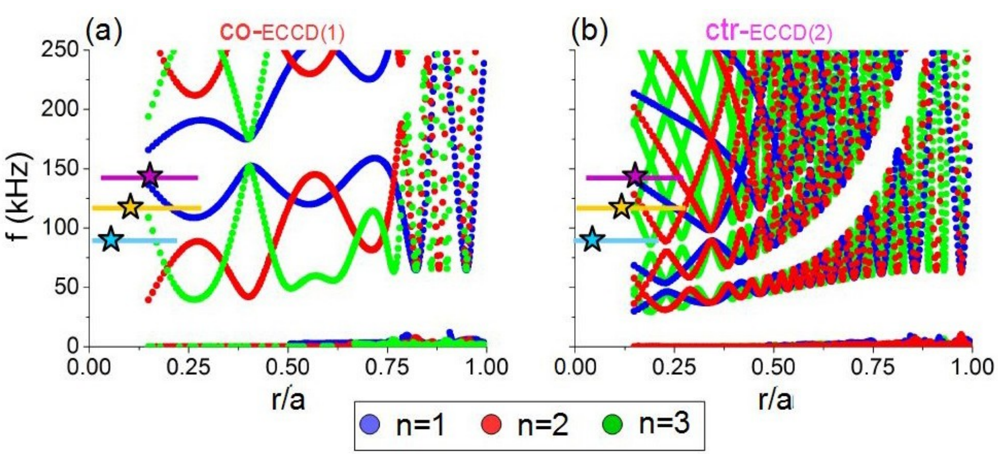

ECH effect in the AE stability of Heliotron J plasma

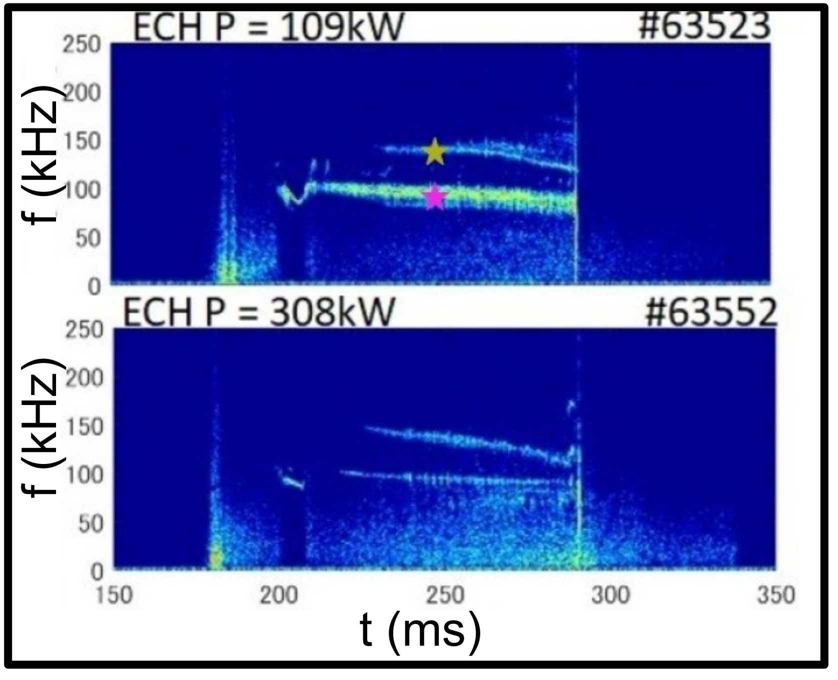

- ECH is applied to stabilize the AE activity in Heliotron J.

- Increase in T_e modifies the EP slowing down time, EP β, plasma resistivity as well as the continuum, FLR and e-i Landau dampings.

- **AE stabilized due to an increase of the dampings !!**

J. Varela et al, Nucl. Fusion, 63, 026009 (2023)

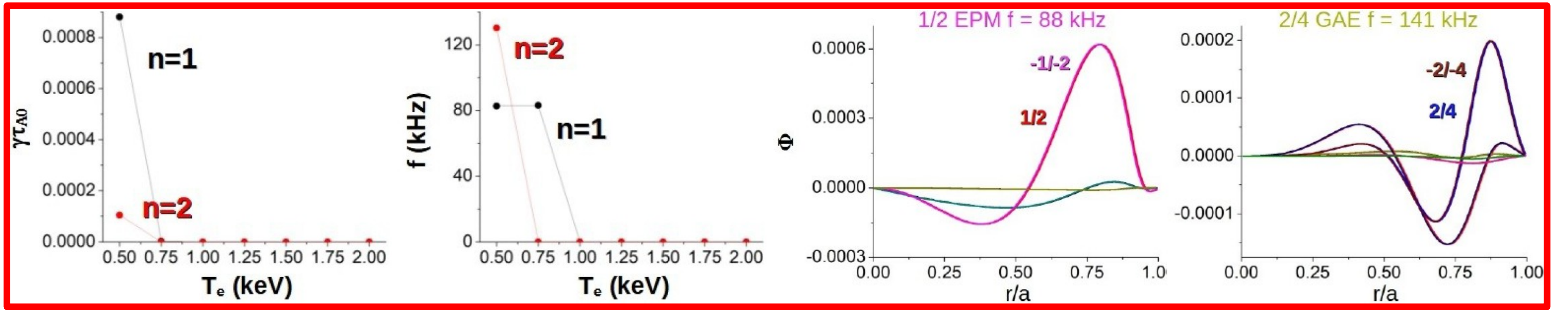

EIC optimization trends in LHD plasma

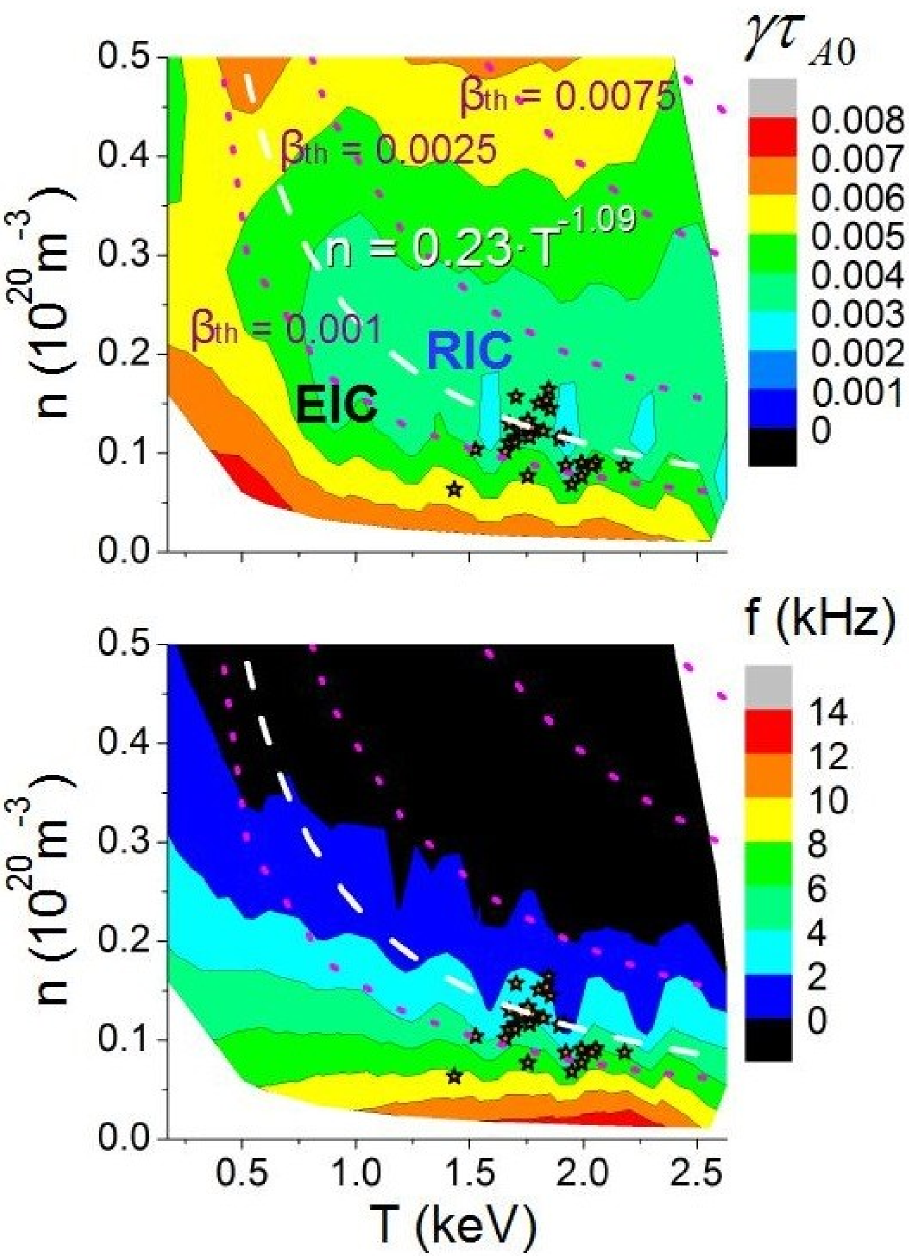

- Energetic-ion-driven resistive interchange mode (EIC) unstable in LHD discharge strongly heated by perpendicular NBI.

- Experimental evidence: EIC stable using off-axis ECH.

- Analysis of EIC stability with respect to the thermal ion density and electron temperature.

- The dashed white line indicates the threshold for EIC destabilization:

$$n = 0.23\,T^{-1.09}$$

- Reasonable agreement with experimental observations (star symbols).

J. Varela et al, 2020 Nucl. Fusion 60 046013

AE modeling and prediction

AE activity in CFQS and QPS device

CFQS

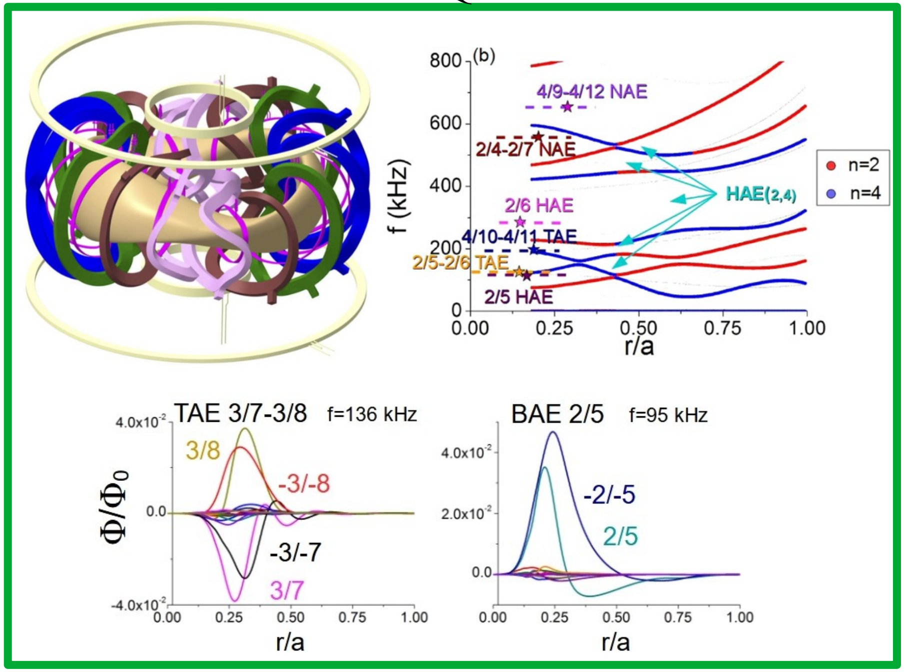

J. Varela *et al Nucl. Fusion* **61** 026023 (2021)

QPS

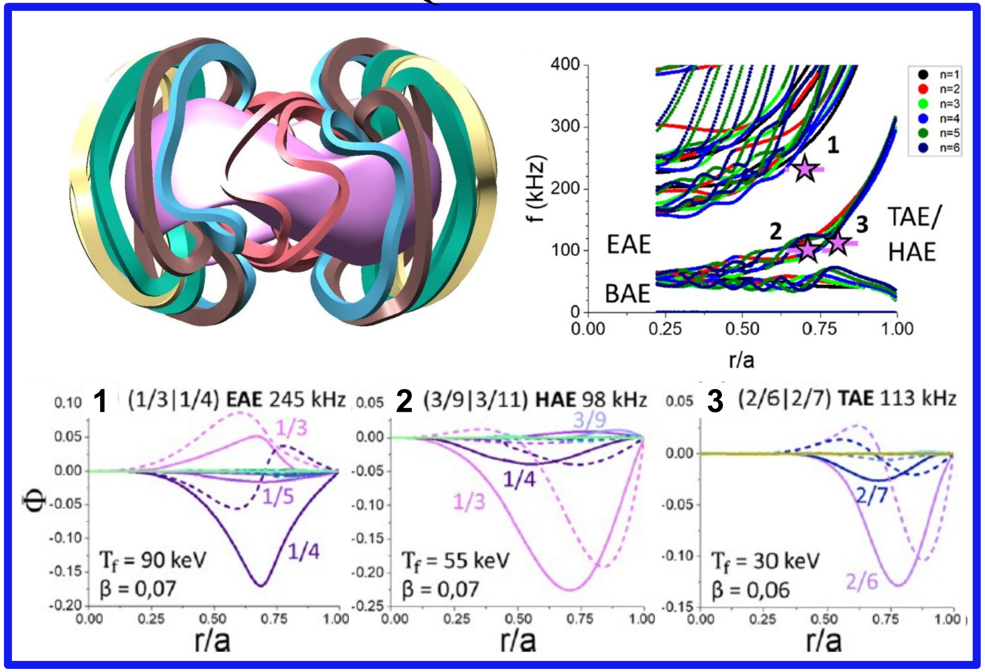

J. Ortiz et al Nucl. Fusion 63 056010 (2023)

- Analysis of the AE stability in magnetic traps with different symmetries.
- First study of AE stability in CFQS and QPS devices
- CFQS first plasma end 2024.

Prediction of AE activity in JT60SA ITER-like inductive scenario

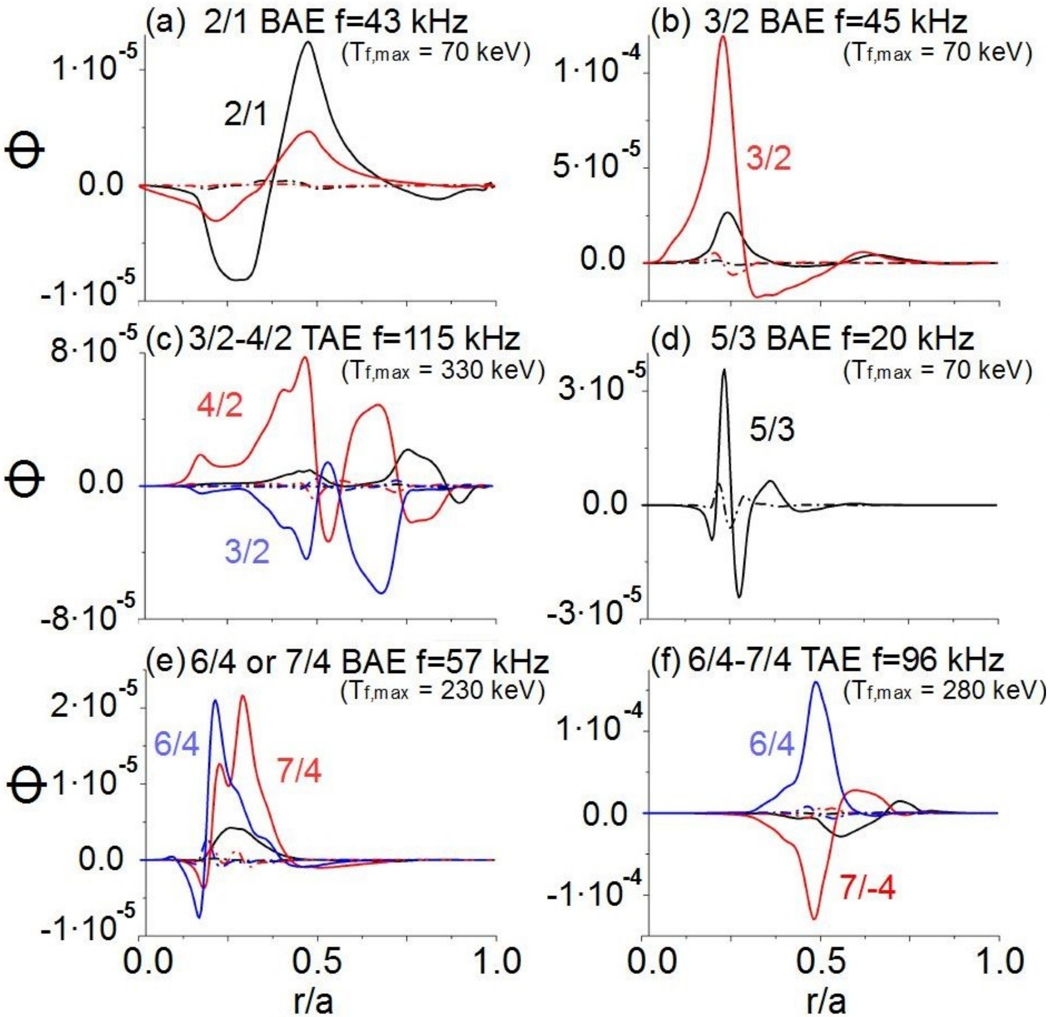

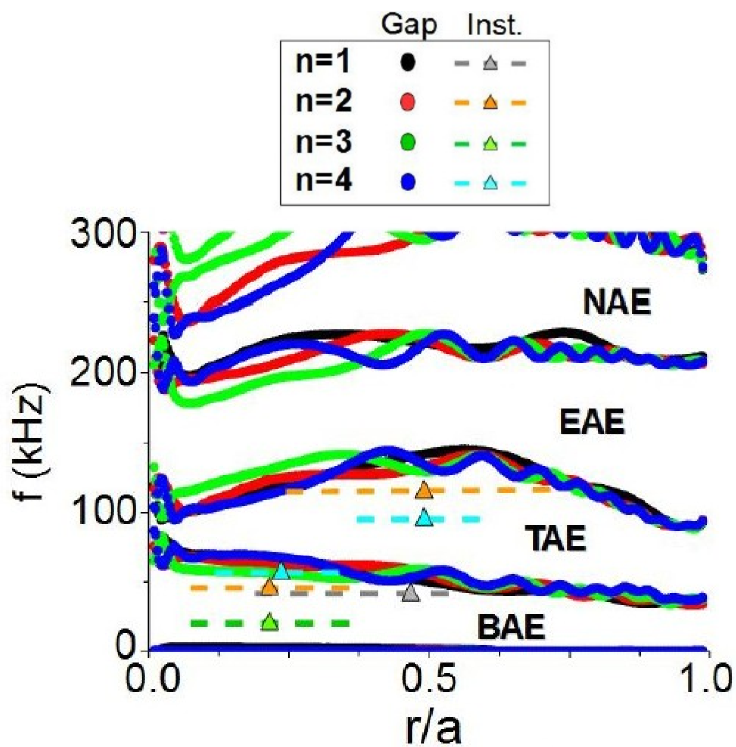

- Marginal unstable n= 1, n=2 and n=3 BAE (triggered by Tf = 70 keV EP).

- Unstable n= 2 and n=4 TAE and n=4 BAE by Tf = 230-330 keV EP.

J. Varela et al, Nucl. Fusion 60 006009 (2020)

Prediction of AE activity in CFETR plasma

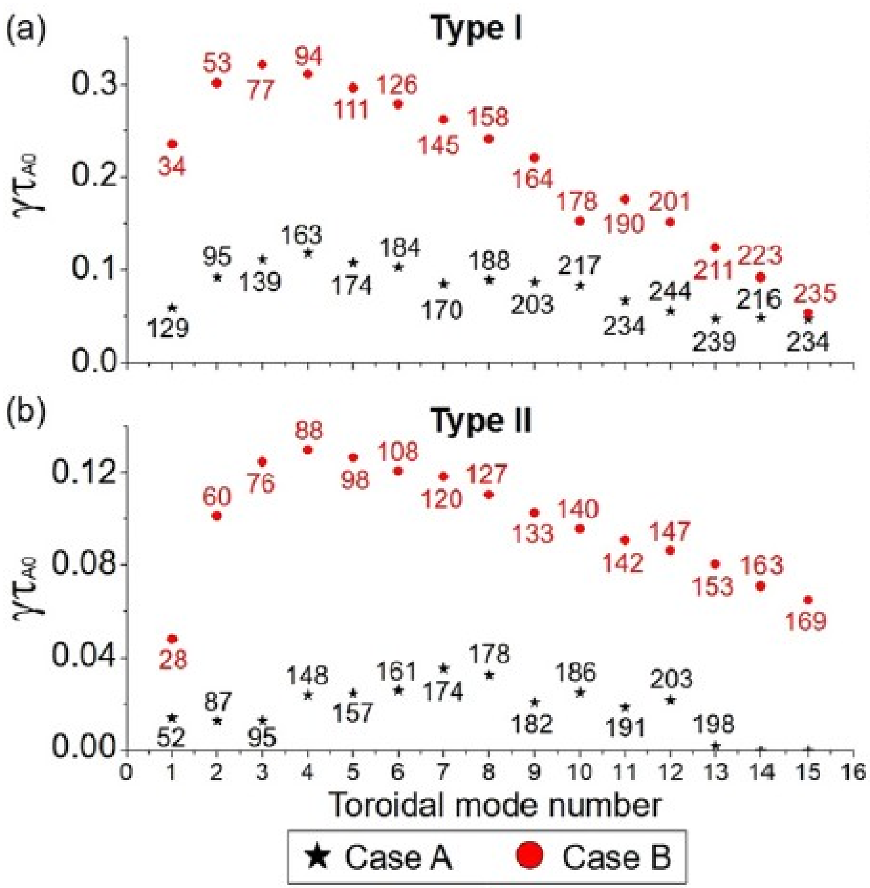

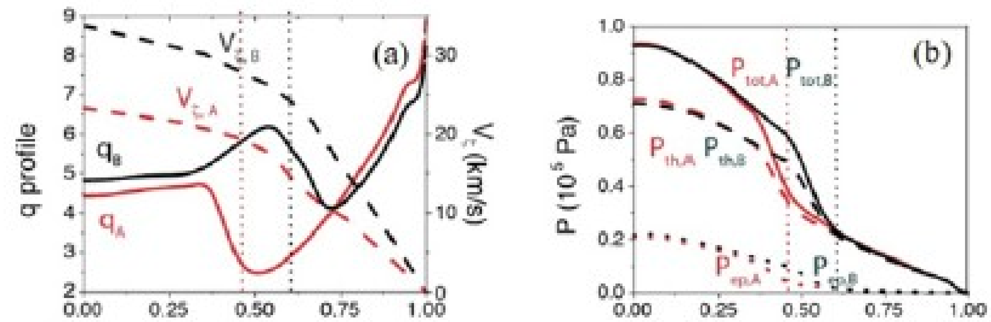

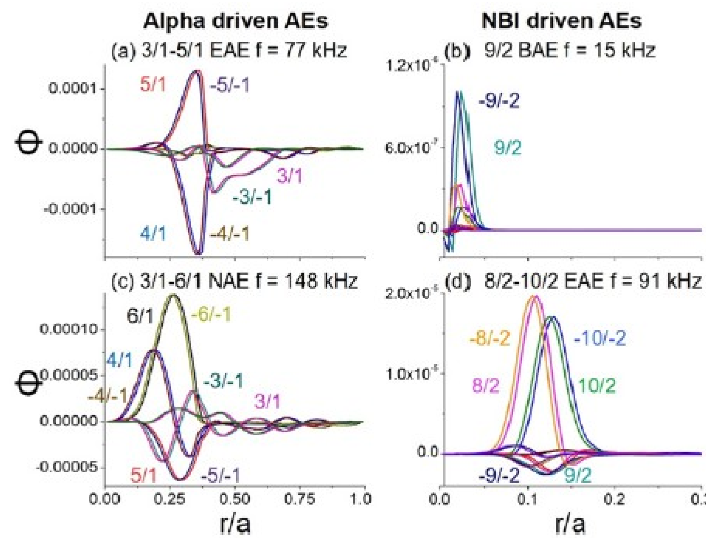

- Strong damping of thermal ion and EP FLR effect: low n modes dominant
- AE stability improves in discharges with the ITB located outward (r/a = 0.6 case B)

J. Varela et al, Nucl. Fusion 62 036005 (2022)

Non linear MHD: Soft-hard MHD transitions

Larger NBI power injection in DIII-D plasma increases the AE activity

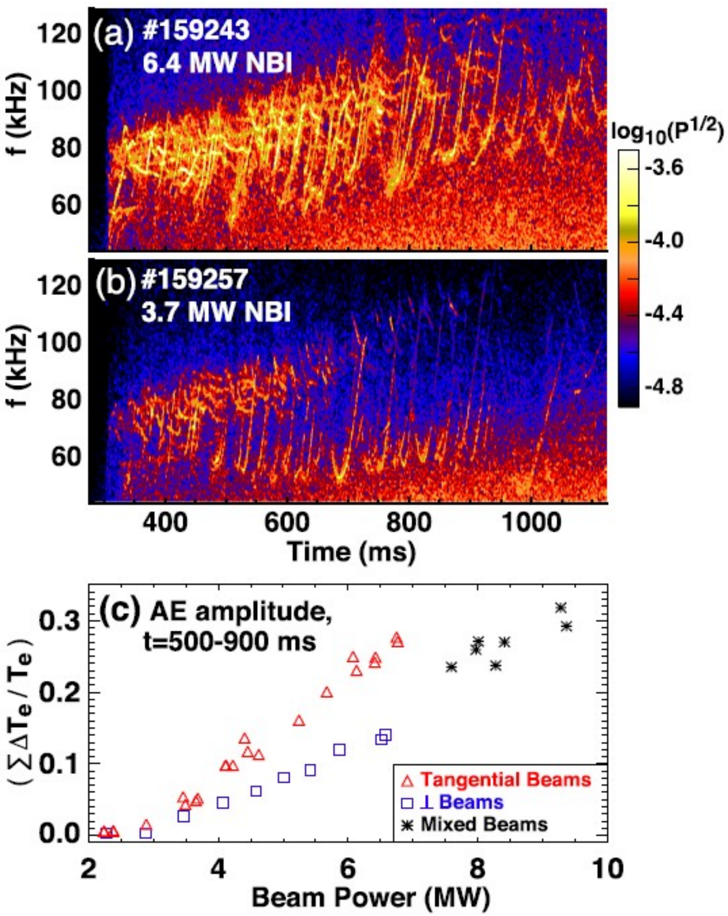

C. S. Collins et al PRL 116, 095001 (2016)

- Stronger NBI power increases the AE activity

- FILD diagnostic measured transient bursts above a given NBI power threshold.

  => hard MHD limit !!

- Higher burst recurrence as the NBI power increases.

- Multiple AE overlapping causes avalanche-like EP transport.

- Stiff EP density profiles: critical gradient model applies !!

Simulations reproduce the burst events

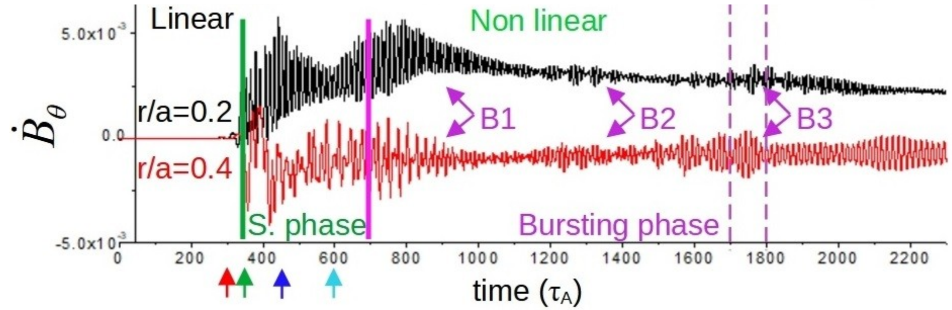

- Burst activity if EP β ≥ 0.02

  => Hard MHD limit transition !!

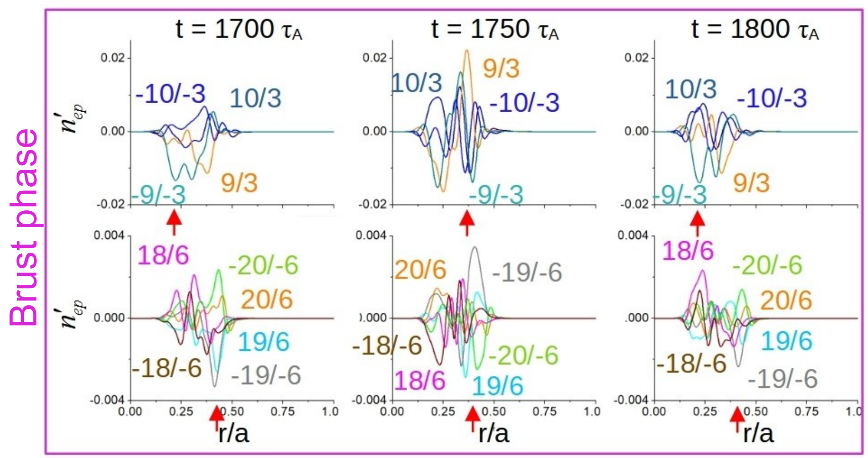

- Burst phase: burst events triggered if n=3 and 6 AEs overlap. NBI operates in the hard MHD limit !!

  => Global plasma relaxation.

  => EP transport increases.

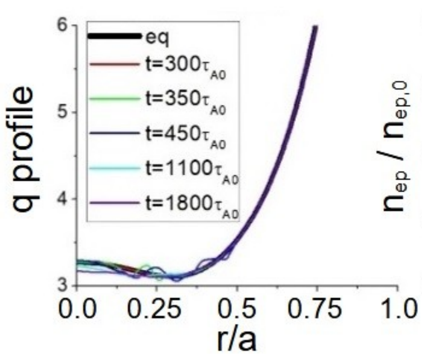

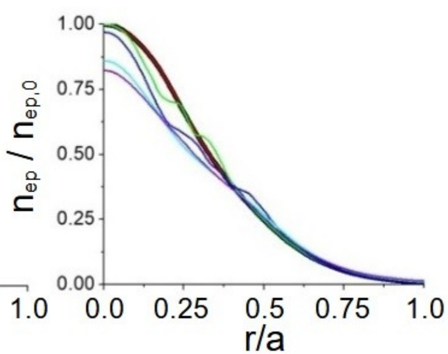

- Large equilibrium profiles perturbation.

=> Enhanced EP transport.

=> Local modification of the magnetic field structure: zonal currents !!

=> Perturbation of the flux surfaces: shear flows !!

J. Varela Plasma Phys. Control. Fusion 65 125004 (2023)

Burst: Critical gradient and EP ballistic transport

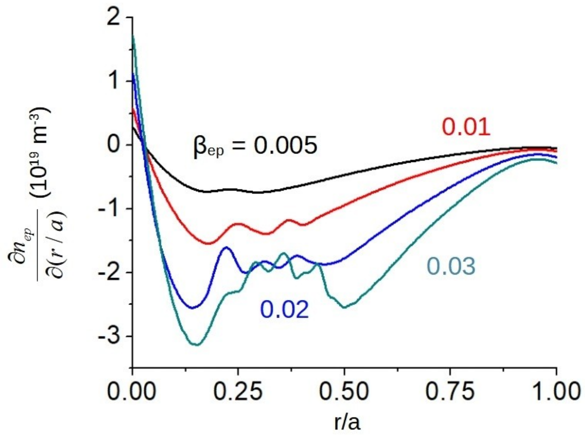

- EP density gradient in soft MHD limit simulations increases with EP β

- **Hard MHD limit simulations show similar EP density gradient !!**

- **Critical gradient-like behavior where bursts are triggered !!**

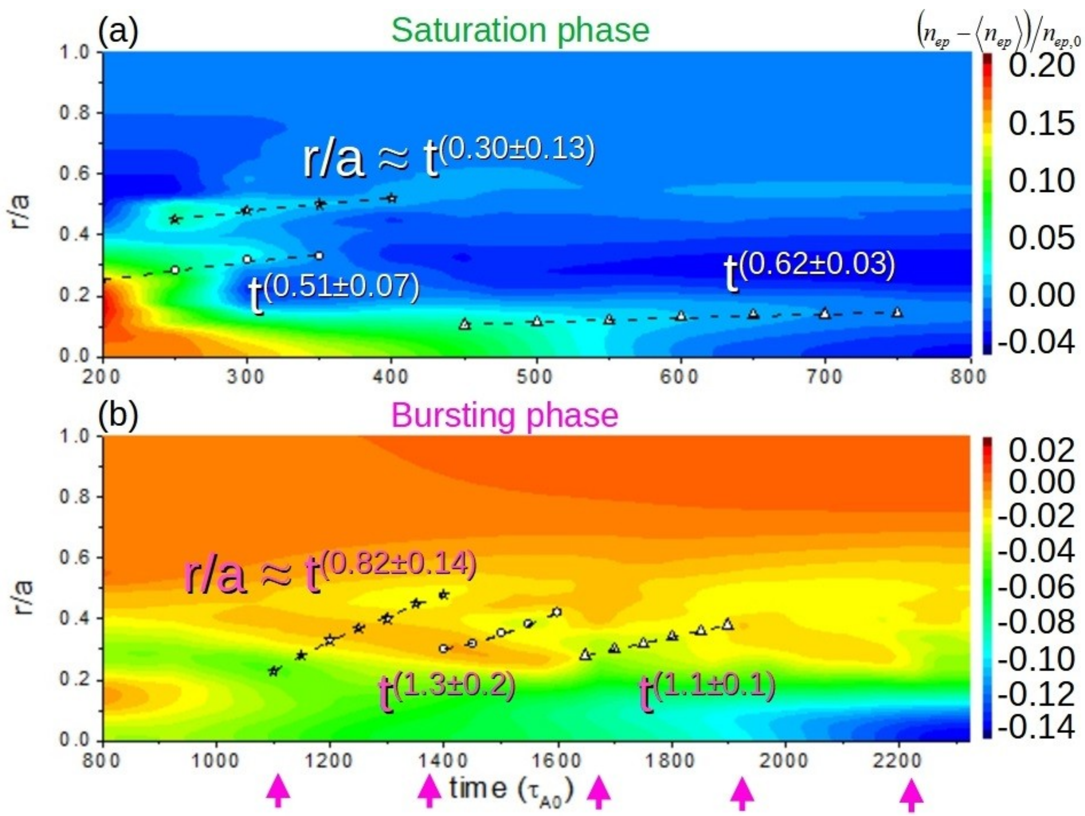

Saturation phase:

- EP diffusive transport: r/a ≈ $t^{1/2}$

Bursting phase:

- EP ballistic transport: r/a ≈ t

=> Avalanche-like events !!

Non linear MHD: Zonal structures

Shear flows generated during MHD and EIC bursts in LHD plasma

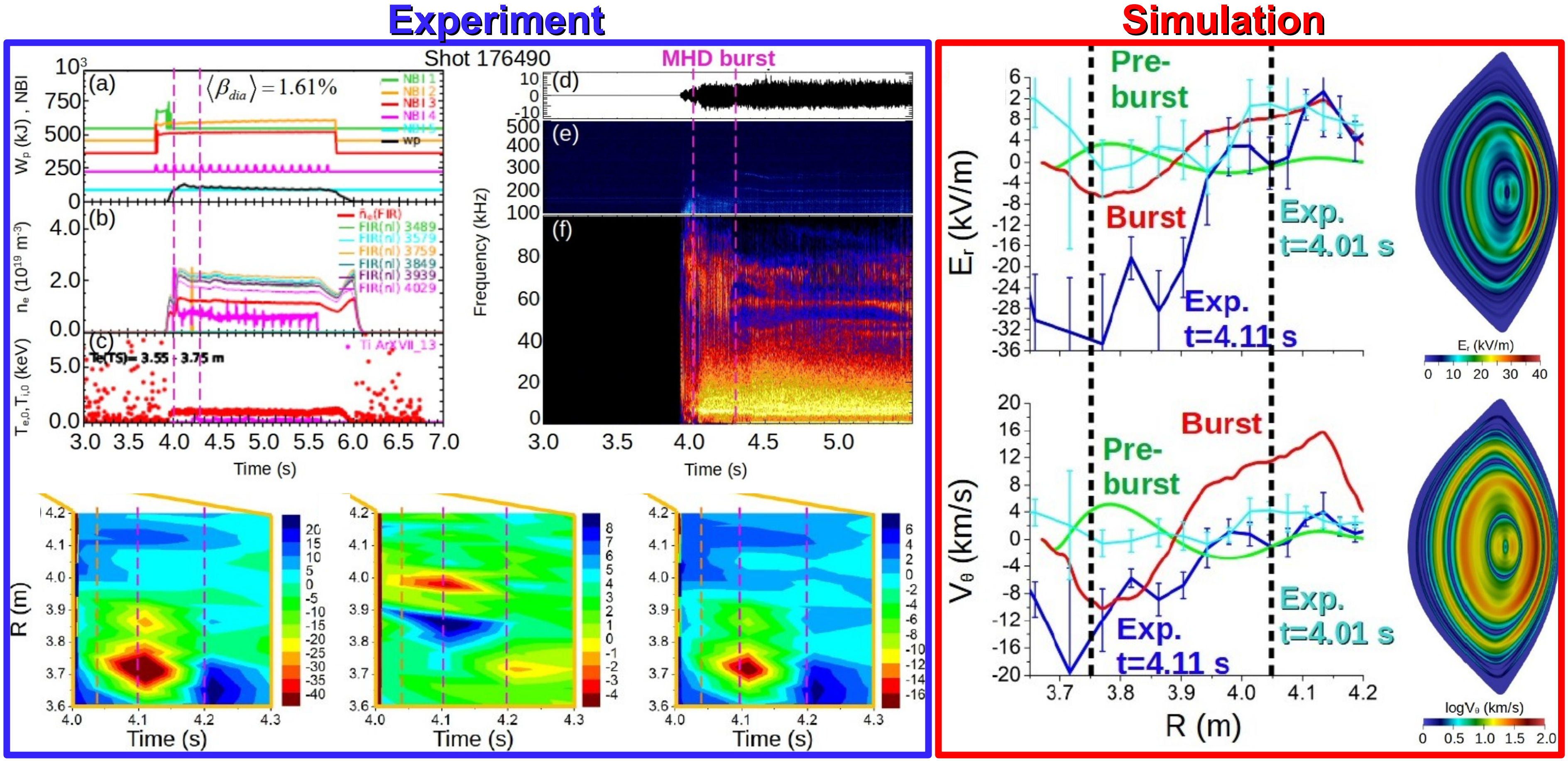

- Shear flows measured by Charge Exchange Spectroscopy.
- Shear flows reproduced in the simulations. Same trends observed.

J. Varela et al, AAPPS-DDP, invited talk 2023

Non linear MHD: thermal plasma instabilities

Internal collapse in LHD plasma

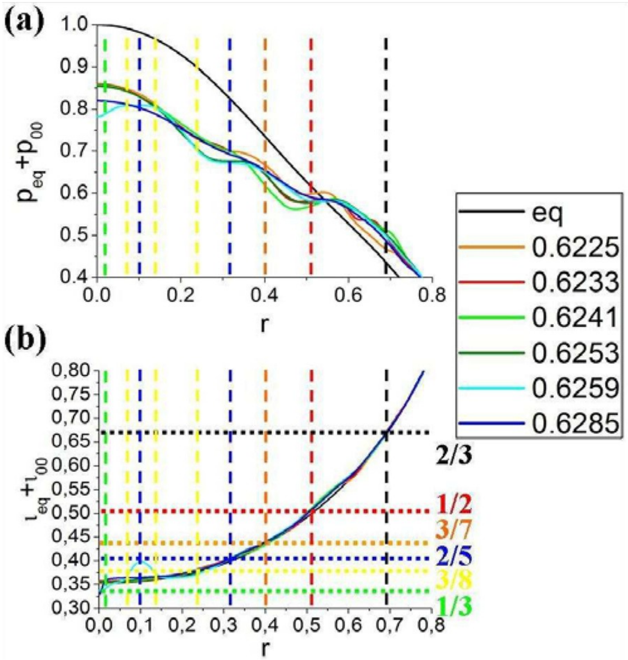

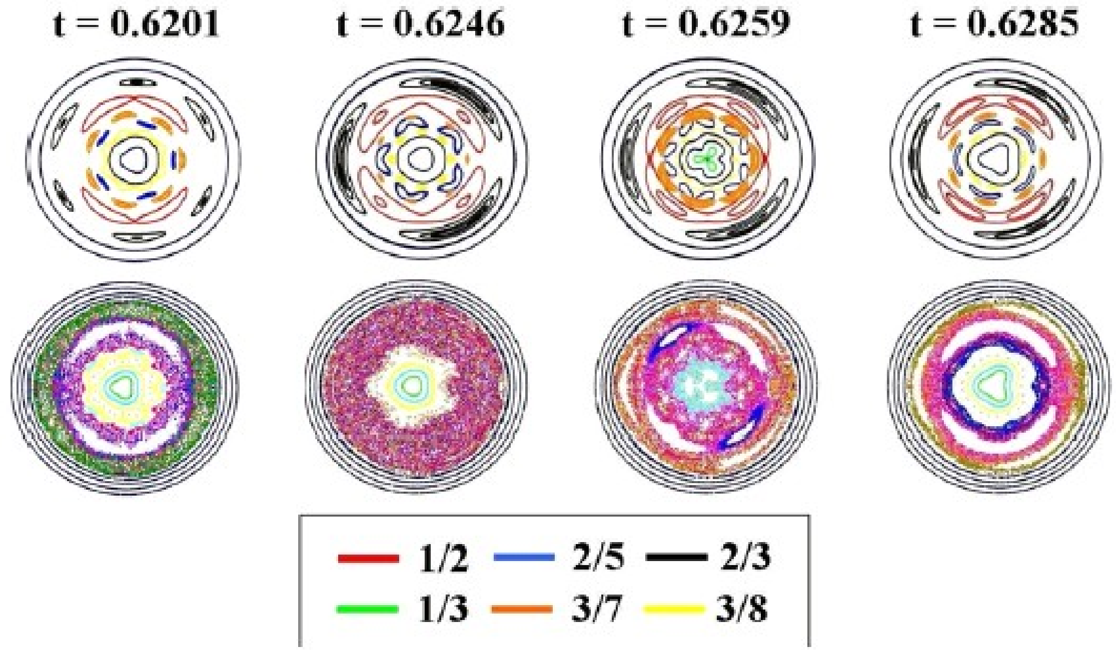

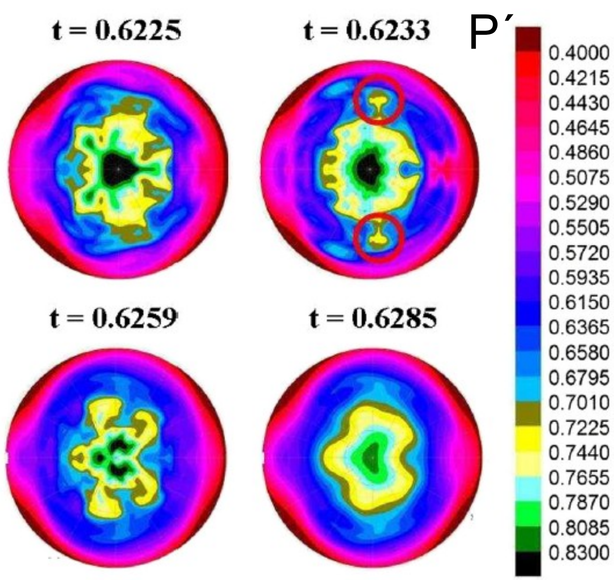

- Large n/m=1/2 magnetic island overlaps with other magnetic islands between the inner-outer plasma.

- Wide stochastic regions appear.

- Flux surfaces rip apart and plasma blobs are expelled to the plasma periphery.

J. Varela et al, 2012 Phys. Plasma 19 082512

J. Varela et al, 2014 Phys. Plasma 21 092505

Sawtooth-like events in LHD plasma

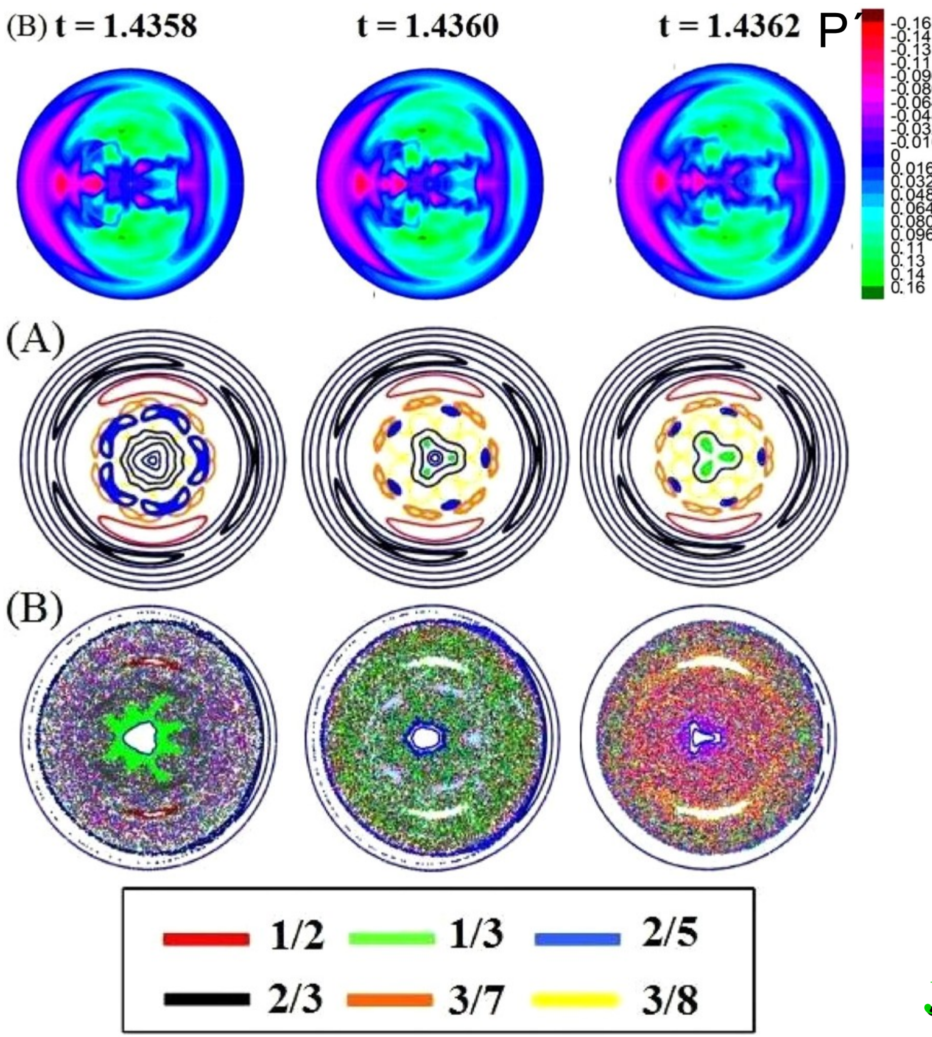

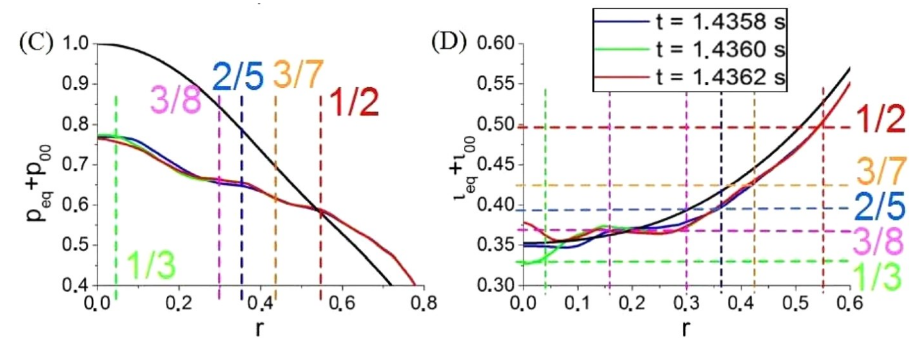

- Zonal current nearby the magnetic axis causes a decrease of the iota profile and n/m=1/3 is resonant.

- Magnetic island of different toroidal families overlap between the inner-middle plasma region.

- A stochastic region appears nearby the magnetic axis.

J. Varela et al, 2012 Phys. Plasma 19 082501

J. Varela et al, 2014 Phys. Plasma 21 032501

Summary

- FAR3d is routinely used to analyze activity of EP driven modes and resistive MHD modes in several nuclear fusion experiments.
- Attached to the experiment: close collaboration with the experimental groups.
- AE characterization and identification of optimization trends.
- Dedicated experiments in LHD, EAST, TJ-II, DIII-D and KSTAR to confirm the optimization trends.
- AE stability prediction in ITER, JT60SA and CFETR plasma.
- More than 40 publications (NF, PPCF and PoP).
- FAR3d code keeps growing !!
- FAR3d review paper submitted.

Last updates

- New FAR3d distribution ver 2.0: public release during November (open source MIT license) includes linear and nonlinear capabilities.

- Helical couplings in nonlinear simulations with 3 EP populations.

- Parallel magnetic field perturbation: internal kinks.

- GPU extension.

- EFIT to code input transformation ad-dons.

- Continuum gaps output.

EXTRA SLICES

FAR3d thermal plasma equations

Toroidal current density

$$J^\zeta = \frac{1}{\rho}\frac{\partial}{\partial\rho}\left(-\frac{g_{\rho\theta}}{\sqrt{g}}\frac{\partial\bar{\psi}}{\partial\theta} + \rho\frac{g_{\theta\theta}}{\sqrt{g}}\frac{\partial\bar{\psi}}{\partial\rho}\right) - \frac{1}{\rho}\frac{\partial}{\partial\theta}\left(\frac{g_{\rho\rho}}{\sqrt{g}}\frac{1}{\rho}\frac{\partial\bar{\psi}}{\partial\theta} + \rho\frac{g_{\rho\theta}}{\sqrt{g}}\frac{\partial\bar{\psi}}{\partial\rho}\right)$$

Ion FLR

$$0 = Q - \nabla_\perp^2\bar{\psi}$$

Two fluid effects: diamagnetic currents

Flow variation along the magnetic field line

$$(1)\quad \frac{\partial\psi}{\partial t} = \frac{\partial\Phi}{\partial\zeta} + \iota\frac{\partial\Phi}{\partial\theta} + \frac{\eta}{S}J_\zeta + \frac{S}{\varepsilon^2}\frac{B_0\rho_i^2}{(J+\iota I)}\left(\frac{V_A^2}{V_{Te}}\right)\left(\frac{\pi}{2}\right)^{1/2}|\nabla_\| Q| + \frac{\Lambda S\beta_0}{2\varepsilon^2\omega_{cy}\sqrt{g}}\left(\frac{\partial p}{\partial\zeta} + \iota\frac{\partial p}{\partial\theta}\right)$$

$$(2)\quad \frac{\partial U}{\partial t} = \frac{S^2\beta_0}{2\varepsilon^2\rho}\left(\frac{\partial\sqrt{g}}{\partial\theta}\frac{\partial p}{\partial\rho} - \frac{\partial\sqrt{g}}{\partial\rho}\frac{\partial p}{\partial\theta}\right) + S^2\left(\frac{\partial J^\zeta}{\partial\zeta} + \iota\frac{\partial J^\zeta}{\partial\theta}\right) + \frac{S^2\beta_f}{2\varepsilon^2\rho}\left(\frac{\partial\sqrt{g}}{\partial\theta}\frac{\partial n_f}{\partial\rho} - \frac{\partial\sqrt{g}}{\partial\rho}\frac{\partial n_f}{\partial\theta}\right) + \frac{S^2\beta_\alpha}{2\varepsilon^2\rho}\left(\frac{\partial\sqrt{g}}{\partial\theta}\frac{\partial n_\alpha}{\partial\rho} - \frac{\partial\sqrt{g}}{\partial\rho}\frac{\partial n_\alpha}{\partial\theta}\right)$$

$$+ S\omega_r\rho_i^2\nabla_\perp^2 U + S\varepsilon^2\frac{\beta_0 V_{th,f}^3}{\omega_{cy}\omega_r}\mathrm{Im}\left[X_e'' + X_i'' - \frac{(X_i' - X_e')}{2 + X_e + X_i} - \upsilon_i(X_i')^2 - \upsilon_e(X_e')^2\right]\Omega_d^2(\Phi) + \frac{S\beta_0(1-\Lambda)}{2\omega_{cy}\varepsilon^2}\left\{\vec{\nabla}\wedge\left[\sqrt{g}\left(\left(\vec{B}\wedge\vec{\nabla}p\right)\cdot\vec{\nabla}\right)\vec{v}_\perp\right]\right\}^\zeta$$

Ion FLR

Pressure gradient driven mode pert.

e-i Landau damping

Toroidal current variation along the magnetic field line

EP density gradient driven mode pert.

Two fluid effects: diamagnetic currents

α density gradient driven mode pert.

FAR3d thermal plasma equations

Advection term

Advection term correction due to the adiabatic index

Acoustic waves: compressibility

Two fluid effects: diamagnetic currents

$$(3)\quad \frac{\partial p}{\partial t} = \frac{dp_{eq}}{d\rho}\frac{1}{\rho}\frac{\partial \Phi}{\partial \theta} + \Gamma p_{eq}\frac{1}{\rho}\left(\frac{\partial \sqrt{g}}{\partial \rho}\frac{\partial \Phi}{\partial \theta} - \frac{\partial \sqrt{g}}{\partial \theta}\frac{\partial \Phi}{\partial \rho}\right) - \frac{\Gamma p_0 B_0}{\varepsilon^2 (J+\tau I)}\left(\frac{\partial}{\partial \theta} + \frac{\partial}{\partial \zeta}\right) v_{\parallel th} + \frac{S\beta_0(1-\Lambda)}{2\omega_{cy}\varepsilon^2\sqrt{g}}\, p\vec{\nabla} p \cdot \left(\vec{\nabla} \wedge \vec{B}\right)$$

$$(4)\quad \frac{\partial v_{\parallel th}}{\partial t} = -\frac{S^2 \beta_0 B_0}{\varepsilon^2 n_0 (J+\tau I)}\left(\frac{\partial}{\partial \zeta} + \tau\frac{\partial}{\partial \theta}\right) p + \frac{1}{\rho}\frac{\partial \psi}{\partial \theta}\frac{dp_{eq}}{d\rho}$$

Compressibility along magnetic field line

Compressibility due to the poloidal flux angular variation

FAR3d: EP equations

EP density between magnetic field lines

EP parallel velocity gradient along the magnetic field line

Flow between different magnetic field lines

Diamagnetic currents generated by flow between different magnetic field line

$$\frac{\partial n_f}{\partial t} = -\frac{v_{th,f}^2}{\varepsilon^2 \Omega_{cy}} \Omega_d\left(n_f\right) - n_{f0} \nabla_{\|} v_{\| f} - n_{f0} \Omega_d\left(\Phi\right) - n_{f0} \Omega\left(\Phi\right)$$

$$+ \left[\frac{\varepsilon^2 \Omega_{cy}}{v_{th,f}^2} \omega_r n_{f0} - \frac{1}{\rho\left(J + \iota I\right)} \frac{dn_{f0}}{d\rho} \left(I \frac{\partial}{\partial \zeta} - J \frac{\partial}{\partial \theta} \right) \right] W_{NBI}$$

EP FLR

Averaged drift velocity operator passing EP

$$\Omega_d = \frac{1}{2B^4\sqrt{g}} \left[\left(\frac{I}{\rho} \frac{\partial B^2}{\partial \zeta} - J \frac{1}{\rho} \frac{\partial B^2}{\partial \theta} \right) \frac{\partial}{\partial \rho} \right]$$

$$- \frac{1}{2B^4\sqrt{g}} \left[\left(\rho \beta_* \frac{\partial B^2}{\partial \zeta} - J \frac{\partial B^2}{\partial \rho} \right) \frac{1}{\rho} \frac{\partial}{\partial \theta} \right]$$

$$+ \frac{1}{2B^4\sqrt{g}} \left[\left(\rho \beta_* \frac{1}{\rho} \frac{\partial B^2}{\partial \theta} - \frac{I}{\rho} \frac{\partial B^2}{\partial \rho} \right) \frac{\partial}{\partial \zeta} \right]$$

Averaged diamagnetic frequency drift

$$\Omega_* = \frac{1}{B^2\sqrt{g}} \frac{1}{n_{f0}} \frac{dn_{f0}}{d\rho} \left(\frac{I}{\rho} \frac{\partial}{\partial \zeta} - J \frac{1}{\rho} \frac{\partial}{\partial \theta} \right)$$

Auxiliary equation

$$0 = (1 - (\rho_{f,\alpha})^2 \nabla_\perp^2) W^{f,\alpha} - (\rho_{f,\alpha})^2 \nabla_\perp^2 \bar{\Phi}$$

FAR3d: EP equations

EP velocity between magnetic field lines

Diamagnetic currents linked to the magnetic field topology

EP density gradient along the magnetic field line

Landau closure: truncate the kinetic moment equation list

$$\frac{\partial v_{\parallel f}}{\partial t} = -\frac{v_{th,f}^2}{\varepsilon^2 \Omega_{cy}} \Omega_d \left(v_{\parallel f} \right) - \frac{v_{th,f}^2}{n_{f0}} \nabla_{\parallel} n_{\parallel f} + v_{th,f}^2 \Omega \left(\psi \right) - \sqrt{\frac{\pi}{2}} v_{th,f} \left| \nabla_{\parallel} v_{\parallel f} \right|$$

$$+ \frac{S v_{th,f}^2}{\rho \left(J + \iota I \right)} \frac{1}{n_{f0}} \frac{d n_{f0}}{d\rho} \left(I X_{1,NBI} - J X_{2,NBI} \right)$$

EP FLR

Auxiliary equations

$$0 = (1 - (\rho_{f,\alpha})^2 \nabla_{\perp}^2) X_1^{f,\alpha} - \frac{\partial \bar{\psi}}{\partial \zeta}$$

$$0 = (1 - (\rho_{f,\alpha})^2 \nabla_{\perp}^2) X_2^{f,\alpha} - \frac{\partial \bar{\psi}}{\partial \theta}$$